Three-dimensional study of reactive diatom-diatom systems: quantum mechanical state-to-state cross sections for the hydrogen-hydroxyl H2 + OX .fwdarw. H + XOH (X = H, D) reactions

ARTICLE *in* THE JOURNAL OF PHYSICAL CHEMISTRY · MAY 2002

Impact Factor: 2.78 · DOI: 10.1021/j100054a018

3 AUTHORS, INCLUDING:

Isidore Last
Tel Aviv University
108 PUBLICATIONS **2,330** CITATIONS
SEE PROFILE

Michael Baer
Hebrew University of Jerusalem
345 PUBLICATIONS **8,264** CITATIONS
SEE PROFILE

Three-Dimensional Study of Reactive Diatom-Diatom Systems: Quantum Mechanical State-to-State Cross Sections for the $H_2 + OX \rightarrow H + XOH$ (X = H, D) Reactions

H. Szichman, I. Last, and M. Baer*

Department of Physics and Applied Mathematics, SOREQ NRC, Yavne 70600, Israel

Received: July 20, 1993®

A detailed quantum mechanical study is made of the three-dimensional tetraatom systems $H_2(\nu_H) + OX(\nu_0) \rightarrow XOH(v'j,v) + H$ (X = H, D). The study is limited to the case where the overall final rotational state K of the product XOH molecules is zero. The calculations are carried out using the negative imaginary arrangement decoupling potentials. The quasi-breathing-sphere approximation is employed for the reagent arrangements and the j_z approximation for the product arrangements. State-to-state and state-selected cross sections are calculated for the (translational) energy range 0.1-0.7 eV.

I. Introduction

In the present work we consider the two isotopic diatom-diatom reactions

$$H_2(\nu_H) + OX(\nu_0) \rightarrow HOX(v'j,v) + H \quad (X = H, D) \quad (I)$$

with the aim of calculating state-to-state reactive cross sections (CS). Numerous experimental[1] and numerical studies[2,3] of those reactions and of the reverse reactions

$$H + HOX(v'j,v) \rightarrow H_2 + OX \quad (II)$$

have been published in the last 15 years. At the beginning of the 1980s Zellner and Steinert[1b] and Chaturvedi and Glass[1c] made experimental studies of reaction I. More detailed experiments on reaction II were carried out at the beginning of the 1990s by Sinha et al.[1e-g] and by Bronikowski and Zare.[1h] Most of these experiments emphasized the effect of the vibrational excitation on the reaction rate. It was found that whereas exciting the reactive bond (namely, the H_2 bond in reaction I or the OH bond in reaction II) strongly enhances the reaction process, exciting the nonreactive bond (the OX bond in both cases) has hardly any effect.

Numerical studies of processes I and II have employed quasi-classical trajectories (QCT)[2a,b,e,f,i] and variational transition-state,[2c] semiclassical,[2a] and quantum mechanical (QM) treatments. Most of these treatments were applied on a potential energy surface calculated by Walch and Dunning[3a] and fitted by Schatz and Elgersma.[2a,3c] Whereas the QCT calculations were carried out without approximations, the QM calculations employed (sometimes even drastic) approximations to reduce the number of internal degrees of freedom. The results of all theoretical treatments to date supported the experimental outcomes; i.e., they indicated that, in the reaction process, there is a strong involvement of the broken bond and a much weaker involvement of the unbroken bond.

We herewith propose a novel three-dimensional (3D) QM treatment of the above tetraatom reactive system. In this treatment the calculations are performed without ignoring any of the six internal coordinates, and in this sense the treatment is fully 3D.

The theory involves an approximation regarding the potential when the reagent molecules are in the region of close proximity. The reagents are assumed to stay in that region for a very short time, so short that the angular part of the potential is hardly allowed to vary. For that short time the behavior of the potential is that of a breathing sphere (namely, not dependent on any angle); the approximation is therefore termed the quasi-breathing-sphere (QBS) approximation. The breathing-sphere potential is formed from the ordinary potential by treating the three reagent Jacobi angles as parameters which are randomly selected by the Monte-Carlo method.[4] The calculations are repeated several times, each time for a different set of three angles. The final outcome follows from an averaging procedure, as will be discussed in the next section.

In addition we employ the negative imaginary potentials (NIP)[5] in order (a) to convert the problem into a bound system problem and permit the application of L^2 basis sets[6a-c] and (b) to decouple unnecessary arrangement channels (AC)[4a,b,d,e] (the tetraatom system in general contains seven open ACs) so that we can consider only the two relevant arrangement channels without the final numerical results being affected.

In this paper we present the detailed theory of our approach. In order to save time, space, and confusion, the theory is carried out for the ground rotational case, namely

$$AB(v_1j_1) + CD(v_2j_2) \rightarrow ABC(v\bar{j}v'|K=0) + D$$

where K is the total rotational quantum number of the product triatom. The same holds for the numerical study; namely, we will report and analyze cross sections (CS) for $K = 0$ only. From preliminary calculations that were carried out for $K \neq 0$ cases, it was found that the state-to-state CSs for $K \neq 0$ are very similar to those of the $K = 0$ case so that the physical content of the $K = 0$ study is quite representative for the general case.

II. Theory

The relevant Schrodinger equation to be considered is[6]

$$(E - H_I)\chi_\lambda = V_\lambda\psi_{0\lambda} \quad (1)$$

where E is the total energy, $\psi_{0\lambda}$ is the λ unperturbed part of the total wave function (henceforth λ designates the atom-triatom AC), V_λ is the relevant perturbation potential, H_I is the full Hamiltonian (which contains the relevant NIPs) defined in the ν AC (henceforth ν designates the diatom-diatom AC), and χ_λ is the function which stands for the perturbed part of the overall wave function Ψ_λ. Thus

$$\chi_\lambda = \Psi_\lambda - \psi_{0\lambda} \quad (2)$$

The aim of the numerical treatment is to obtain the state-to-state S matrix element[7]

$$S(\nu \rightarrow \lambda) = \langle\psi_{0\nu}|V_\nu|\Psi_\lambda\rangle = \langle\psi_{0\nu}|V_\nu|(\chi_\lambda + \psi_{0\lambda})\rangle \quad (3)$$

where $\psi_{0\nu}$ is the ν unperturbed wave function and V_ν is the relevant perturbation potential in this AC.

* Abstract published in *Advance ACS Abstracts*, December 15, 1993.

0022-3654/94/2098-0828$04.50/0

To obtain $S(\nu \rightarrow \lambda)$, it is necessary to carry out the following steps.

II.1. Derivation of the Unperturbed Wave Functions $\psi_{0\alpha}$ (α = λ, ν). To derive $\psi_{0\alpha}$ ($\alpha = \lambda, \nu$), we consider the unperturbed Hamiltonian $H_{0\alpha}$ and the relevant Schrodinger equation (SE)

$$(E - H_{0\alpha})\psi_{0\alpha} = 0 \quad (\alpha = \lambda, \nu) \tag{4}$$

$H_{0\alpha}$ is written in the form

$$H_{0\alpha} = T_\alpha + W_\alpha \quad (\alpha = \lambda, \nu) \tag{5}$$

where T_α is the kinetic energy and W_α is the unperturbed potential. Since different clusters are encountered in the two ACs, we discuss each equation (and solution) separately.

II.1.1. Reagent Equation ($\alpha = \nu$). Here two diatoms are encountered, and consequently T_ν takes the form

$$T_\nu = -\frac{\hbar^2}{2\mu_1 r_1}\frac{\partial^2}{\partial r_1^2} r_1 - \frac{\hbar^2}{2\mu_2 r_2}\frac{\partial^2}{\partial r_2^2} r_2 - \frac{\hbar^2}{2\mu_\nu R_\nu}\frac{\partial^2}{\partial R_\nu^2} R_\nu + \frac{\hbar^2}{2\mu_1}\frac{j_1(j_1+1)}{r_1^2} + \frac{\hbar^2}{2\mu_2}\frac{j_2(j_2+1)}{r_2^2} + \frac{\vec{l}_\nu^{\,2}}{2\mu_\nu R_\nu^2} \tag{6}$$

Here μ_i, r_i, and j_i ($i = 1, 2$) are the reduced masses, the vibrational coordinates, and the internal rotational quantum numbers, respectively, of the two diatomics, μ_ν is the νth reduced mass, R_ν the νth translational coordinate, and $\vec{l}_\nu$ is the orbital angular momentum operator. If $\vec{J}_\nu$ is defined as

$$\vec{J}_\nu = \vec{j}_1 + \vec{j}_2 \tag{7}$$

and if $\vec{J}$ is the total angular momentum (operator) of the system, then $\vec{l}_\nu$ is written as

$$\vec{l}_\nu = \vec{J} - \vec{J}_\nu \tag{8}$$

Henceforth we shall employ the body-fixed (BF) framework, in which the z axis is assumed to be along $\vec{R}_\nu$. Next, we introduce the j_z approximation,[8] and consequently the scalar representation of $\vec{l}_\nu^{\,2}$ is

$$\vec{l}_\nu^{\,2} \equiv \hbar^2(J(J+1) - 2\Omega_\nu^2) + \vec{J}_\nu^{\,2} \tag{9}$$

where Ω_ν is the projection of both J and J_ν along R_ν. To evaluate J_ν^2, we apply once more the j_z approximation,[8] i.e., $\vec{J}_\nu^{\,2}$ will be presented as

$$\vec{J}_\nu^{\,2} = \hbar^2(j_1(j_1+1) + j_2(j_2+1) - 2m_1m_2) \tag{10}$$

where m_i ($i = 1, 2$) are the projections of j_i ($i = 1, 2$), respectively, along R_ν. It can be seen that

$$\Omega_\nu = m_1 + m_2 \tag{11}$$

As for W_ν it is assumed to be of the form[9]

$$W_\nu(r_1 r_2 R_\nu \gamma_1 \gamma_2 \delta) = v_1(r_1) + v_2(r_2) + w_\nu(R_\nu) \tag{12}$$

where $v_i(r_i)$ ($i = 1, 2$) are the asymptotic vibrational potentials of the two diatoms, $w_\nu(R_\nu)$ is the νth distortion potential (assumed to increase once R_ν is small enough and decreases), γ_i ($i = 1, 2$) are two Jacobi angles defined as

$$\gamma_i = \cos^{-1}(\hat{R}_\nu \cdot \hat{r}_i) \quad (i = 1, 2) \tag{13}$$

and δ is the angle between the $(\hat{R}_\nu, \hat{r}_1)$ and $(\hat{R}_\nu, \hat{r}_2)$ planes. The potential $w_\nu(R_\nu)$ is usually taken as

$$w_\nu(R_\nu) = U(r_{1e} r_{2e} R_\nu \gamma_{10} \gamma_{20} \delta_0) \tag{14}$$

where U is the full potential expressed in terms of the νth coordinates, r_{ie} ($i = 1, 2$) are diatomic asymptotic equilibrium distances and γ_{i0} ($i = 1, 2$) and δ_0 are three fixed angles to be discussed later.

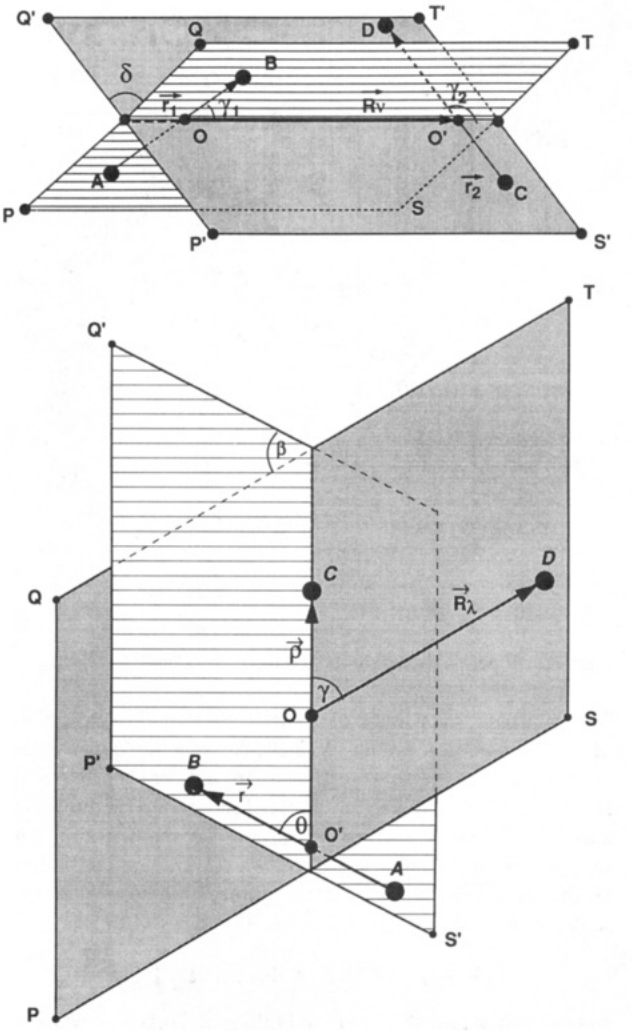

Figure 1. Jacobi coordinates of the four-atom system: (a, top) reagent (diatom–diatom) coordinates, (b, bottom) product (atom–triatom) coordinates.

Since the W_ν potential is separable in terms of all variables, the solution of eq 4 can be written as

$$\psi_{0\nu}^{(i)}(r_1 r_2 R_\nu \gamma_1 \gamma_2 \delta | t_1 t_2 J) = (1/r_1 r_2 R)\phi_{0\nu}^{(1)}(r_1|t_1)\,\phi_{0\nu}^{(2)}(r_2|t_2) \times \zeta_{0\nu}(R_\nu|t_1 t_2 J)\, y(\gamma_1\delta_1|t_1)\, y(\gamma_2\delta_2|t_2) \tag{15}$$

where $\phi_{0\nu}(r_i|t_i)$ ($i = 1, 2$) are the νth vibrational eigenfunctions, $y(\gamma_i\delta_i|t_i)$ are the respective spherical harmonics, $\zeta_{0\nu}(R_\nu|t_1 t_2 J)$ is the corresponding translational function, and t_i ($i = 1, 2$) stand for the three quantum numbers n_i, j_i, and m_i. Here n_i and j_i are vibrational and rotational quantum numbers and m_i is the z component of j_i with respect to R_ν (the νth BF z axis). As for δ_i ($i = 1, 2$), the final results will depend only on $\delta = \delta_2 - \delta_1$ (the Jacobi coordinates for the two interacting diatoms are shown in Figure 1a).

II.1.2. Product Equation ($\alpha = \lambda$). In the case of $\alpha = \lambda$ one encounters an atom and a triatom, and consequently T_λ becomes

$$T_\lambda = -\frac{\hbar^2}{2mr}\frac{\partial^2}{\partial r^2} r - \frac{\hbar^2}{2\mu\rho}\frac{\partial^2}{\partial \rho^2}\rho - \frac{\hbar^2}{2\mu_\lambda R_\lambda}\frac{\partial^2}{\partial R_\lambda^2} R_\lambda + \frac{\vec{j}^{\,2}}{2mr^2} + \frac{(\vec{K} - \vec{j})^2}{2\mu\rho^2} + \frac{\vec{l}_\lambda^{\,2}}{2\mu_\lambda R_\lambda^2} \tag{16}$$

Here m and μ are the reduced masses of one reagent diatom (say AB; see Figure 1) and of the triatom (ABC), respectively, r is the vibrational coordinate of AB ($r \equiv r_1$), ρ is the corresponding

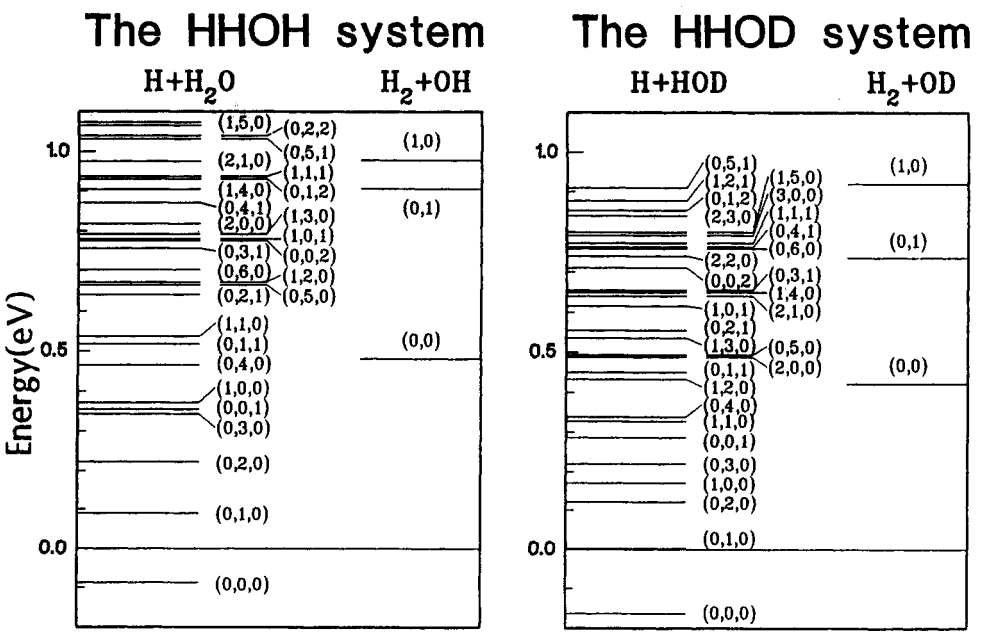

Figure 2. Eigenstates for the HHOH and the HHOD systems.

"translational" coordinate of the triatom, μ_λ is the reduced mass of the atom–triatom system, R_λ is the corresponding translational coordinate, $\vec{j}$ is the rotational angular momentum of AB with respect to C, $\vec{K}$ is the total angular momentum of the triatom, and $\vec{l}_\lambda$ is the corresponding orbital angular momentum. Again the j_z approximation[8] is employed twice. First ρ is considered to be the BF z axis for the triatom system, and consequently the scalar representation of $(\vec{K}-\vec{j})^2$ is[10]

$$(\vec{K}-\vec{j})^2 \equiv \hbar^2[(K(K+1)-2\Omega_k^2]+\vec{j}^2 \qquad (17)$$

where Ω_k is the projection of $\vec{K}$ and $\vec{j}$ along $\hat{\rho}$. Next $\hat{R}_\lambda$ is considered to be the BF z axis for the atom–triatom system, and consequently the scalar representation of $\vec{l}_\lambda^2$ is

$$\vec{l}_\lambda^{\,2} \equiv \hbar^2[J(J+1)+K(K+1)-2\Omega_\lambda^2] \qquad (18)$$

where Ω_λ is the projection of both K and J along R_λ.

As for W_λ, it is assumed to be of the form

$$W_\lambda(r\rho R_\lambda\theta\beta\gamma) = v(r\rho\theta)+w_\lambda(R_\lambda) \qquad (19)$$

where $v(r\rho\theta)$ is the potential of the isolated triatom, $w_\lambda(R_\lambda)$ is the λth distortion potential which is assumed to increase once R_λ is small enough and decreases, and θ and β are the spherical angles relating $\hat{r}$ to $\hat{\rho}$; in particular θ is defined as

$$\theta = \cos^{-1}(\hat{r}\cdot\hat{\rho}). \qquad (20)$$

The potential $w_\lambda(R_\lambda)$ is usually taken as

$$w_\lambda(R_\lambda) = U(R_\lambda\rho_e r_e\theta_e\gamma_0\beta_0) \qquad (21)$$

where U again is the full potential, this time expressed in terms of λ coordinates, and r_e, ρ_e, and θ_e are the equilibrium coordinates for the triatom. β and γ are two spherical coordinates relating $\vec{\rho}$ to $\vec{R}_\lambda$; in particular γ is the angle between $\hat{R}_\lambda$ and $\hat{\rho}$, namely

$$\gamma = \cos^{-1}(\hat{R}_\lambda\cdot\hat{\rho}) \qquad (22)$$

β and γ are fixed angular values which serve as parameters, and the final results are expected not to be dependent on them (the same as for r_e, ρ_e, and θ_e). The Jacobi coordinates for the interacting atom–triatom system are shown in Figure 1b.

In what follows we assume that $\vec{K} \equiv 0$ and consequently also $\Omega_K = \Omega_\lambda = 0$. Since the W_λ potential is separable, the solution of eq 4 can be written as

$$\psi_{0\lambda}(r\rho R_\lambda\theta\beta\gamma|vjv'J) = (1/r\rho R_\lambda)\phi_\lambda(r\rho\theta|v\bar{j}v')\,\zeta_{0\lambda}(R_\lambda|vjv'J) \qquad (23)$$

where $\phi_\lambda(r\rho\theta|vjv')$ are the eigenfunctions of the equation[10]

$$\left[-\frac{\hbar^2}{2m}\frac{\partial^2}{\partial r^2}-\frac{\hbar^2}{2\mu}\frac{\partial^2}{\mu\rho^2}+\frac{\vec{j}^2}{2}\left(\frac{1}{mr^2}+\frac{1}{\mu\rho^2}\right)+ v(r\rho\theta)-\epsilon(v\bar{j}v')\right]\phi_\lambda(r\rho\theta|v\bar{j}v')=0 \qquad (24)$$

and $\zeta_{0\lambda}(R_\lambda|vjv'J)$ are the solutions of the equation

$$\left[-\frac{\hbar^2}{2\mu_\lambda}\frac{\partial^2}{\partial R_\lambda^2}+w_\lambda(R_\lambda)+\frac{\hbar^2}{2\mu_\lambda}\frac{J(J+1)}{R_\lambda^2}- \frac{\hbar^2}{2\mu_\lambda}k^2(v\bar{j}v')\right]\zeta_{0\lambda}(R|v\bar{j}v'J)=0 \qquad (25)$$

Here $\epsilon(v\bar{j}v')$ are eigenvalues and $k(v\bar{j}v')$ is defined as

$$k(v\bar{j}v') = [(2\mu_\lambda/\hbar^2)(E-\epsilon(v\bar{j}v'))]^{1/2} \qquad (26)$$

The eigenvalues for this (the product) AC as well as for the reagent AC are presented in Figure 2.

In the general case when $K \neq 0$, the expression in eq 23 should be multiplied by $\mathbf{d}^K_{\Omega_K\Omega_\lambda}(\gamma)$, the representation of the rotation matrix with respect to the $\hat{R}_\nu$ axis.[13]

II.2. Derivation of the Perturbed Function χ_λ. The function χ_λ is derived by solving eq 1 in the ν AC (the AC of the two interacting diatoms). For this sake the ν AC is enlarged significantly by extending the range of the reagent vibrational coordinate(s) into the corresponding reactive AC(s). In our particular case only one reactive bond is encountered, namely, the H_2 bond; consequently, as will be seen, the calculations are carried out for an extended range of the H_2 vibrational coordinate r_1, i.e., $0.4 \le r_1 \le 3.2$ Å.

The Hamiltonian H_I in eq 1 will be written in the form

$$H_I = T_\nu + U(\vec{R}_\nu\vec{r}_1\vec{r}_2)+V_I(R_\nu r_1 r_2) \qquad (27)$$

where T_ν is the kinetic energy operator, U is the QBS potential expressed in terms of the ν coordinates, and $V_I(R_\nu r_1 r_2)$ is the required NIP to be discussed later. Henceforth we assume $U(R_\nu r_1 r_2)$ to be dependent on only the three Jacobi distances R_ν,

r_1, and r_2. A potential like this one is obtained by treating the three internal Jacobi angles γ_1, γ_2, and δ as parameters and not as variables. Consequently,

$$U(R_\nu r_1 r_2) = U(R_\nu r_1 r_2|\gamma_1=\gamma_{10},\gamma_2=\gamma_{20},\delta=\delta_0) \quad (28)$$

It follows that each calculation is to be carried out for fixed values of these angles but that the overall numerical treatment is to be done for several Monte-Carlo randomly selected sets of these angles. As for T_ν, it is assumed to be identical to that presented in eq 6, with the additional definitions given in eqs 9–14. It is important to emphasize that within the QBS the two quantum numbers j_1 and j_2 do not change and remain identical to their asymptotic values.

As already mentioned, the third term in eq 27 is the NIP. The NIP is made up of several terms. They number $M + 1$ at most, M being the number of reactive bonds. In our case, in the ν AC, two bonds, the H_2 and the OH bonds, are encountered; of these only the H_2 bond is reactive (for energies below breakup). Consequently two negative imaginary terms are to be added to the real Hamiltonian: a vibrational term iv_{1r}, and the translational term iv_{1R}. Thus

$$V_1(R_\nu r_1 r_2) \equiv -i(v_{1r}(r_1) + v_{1R}(R)) \quad (29)$$

The potentials are assumed to be the Neuhauser–Baer (BN) linear ramp potentials:[5]

$$V_{1x}(x) = \begin{cases} v_{10x}\dfrac{x - x_1}{\Delta x_1}; & x_1 \le x \le x_1 + \Delta x_1 \\ 0; & \text{otherwise} \end{cases} \quad (30)$$

Here x_1 is a point in the asymptotic region, Δx_1 is the range along which $V_{1x} \neq 0$ and V_{10x} is the height of the potential. The two parameters Δx_1 and V_{10x} are determined according to the BN inequalities.[5]

Returning to eq 1 (and eq 3), it is noticed that V_λ (and V_ν) must still be presented explicitly. In both cases V_α ($\alpha = \lambda, \nu$) are defined as

$$V_\alpha = U - W_\alpha \quad (\alpha = \lambda, \nu) \quad (31)$$

where W_ν and W_λ are given in eqs 12 and 19, respectively.

We continue to describe the derivation of χ_λ. Since the whole treatment is to be carried out in the ν AC for a given fixed set of three Jacobi angles (γ_1, γ_2, δ), we shall omit the index ν and any references to these angles.

Adding the two NIPs to the real potential U converts the scattering problem into a bound system problem, and consequently χ_λ can be expanded in terms of square integrable L^2 functions.[6,11] The ones we chose are localized functions for the translational components and adiabatic basis sets related to the two vibrational coordinates.[12]

To continue, we shall refer to a simplified case, where $m_1 = m_2 = 0$. Consequently χ_λ will be written as

$$\chi_\lambda{}^J(Rr_1r_2|j_1j_2|vjv') = (Rr_1r_2)^{-1}\sum_{qt} a^J(vjv'|j_1j_2|qt)\, g(R|q)\, f(r_1r_2|j_1j_2|qt) \quad (32)$$

Here $g(R|q)$ is the localized Gaussian function:[12]

$$g(R|q) = \left(\frac{\alpha}{\sigma\pi^{1/2}}\right)^{1/2} \exp\left[-\frac{\alpha^2}{2}\left(\frac{R - R_q}{\sigma}\right)^2\right] \quad (33)$$

where R_q ($q = 0, ..., N$) are equidistant division points along the interval $[0, R_1 + \Delta R_1]$, α is a dimensionless parameter, and σ is the grid size

$$\sigma = R_q - R_{q-1} \quad (34)$$

$f(r_1r_2|j_\nu|qt)$ is an eigenfunction of the equation

$$\left[-\frac{\hbar^2}{2\mu_1}\frac{\partial^2}{\partial r_1{}^2} - \frac{\hbar^2}{2\mu_2}\frac{\partial^2}{\partial r_2{}^2} + U(r_1r_2R=R_q) + \frac{\hbar^2}{2}\left(\frac{j_1(j_1+1)}{\mu_1 r_1{}^2} + \frac{j_2(j_2+1)}{\mu_2 r_2{}^2}\right) - \epsilon(t|j_1j_2|R_q)\right] f(r_1r_2|j_1j_2|qt) = 0 \quad (35)$$

where $\epsilon(t|j_1j_2|R_q)$ is the corresponding eigenvalue (t is the integer quantum number related to the eigenstate of eq 35).

The $a^J(vjv'|j_1j_2|qt)$ coefficients will be obtained following the substitution of eqs 32, 27, and 23 into eq 1 and from the solution of the relevant system of algebraic equations:

$$(\mathbf{A}^J - i\mathbf{B})\mathbf{a}^J = \mathbf{Z}^J \quad (36)$$

where

$$A^J_{qtq't'}(j_1j_2) = \langle g(R_\nu|q)\, f(r_1r_2|j_1j_2|qt)|E - H|g(R_\nu|q')\, f(r_1r_2|j_1j_2|q't')\rangle \quad (37a)$$

$$Z^J_{tq}(vjv'j_1j_2) = \int\int\int \mathbf{d}^J_{00}(\Delta)(r_1r_2R_\lambda/r\rho R_\nu)\mathrm{d}r_1\, \mathrm{d}r_2\, \mathrm{d}R_\nu \times g(R_\nu|q)\, f(r_1r_2|j_1j_2|qt)\, V_\lambda(r\rho R_\lambda\theta\gamma\beta)\, \phi_\lambda(r\rho\theta|v\bar{j}v')\, \zeta_{0\lambda}(R_\lambda|v\bar{j}v'J) \quad (37b)$$

and

$$B_{qtq't'}{}^{(j_1j_2)} = \langle g(R_\nu|q)\, f(r_1r_2|j_1j_2|qt)|(v_{1r}(r_1) + v_{1R}(R_\nu))|g(R_\nu|q')\, f(r_1r_2|j_1j_2|q't')\rangle \quad (37c)$$

Here H is the full (real) Hamiltonian, $\mathbf{d}^J_{00}$ is the representation of the rotation matrix with respect to the R_ν axis,[13] and Δ is the polar angle between R_ν and R_λ. It is important to mention that in the general case the integrand in eq 37b has to be multiplied by $\mathbf{d}^J_{\Omega_\nu\Omega_\lambda}(\Delta)$ where Ω_ν and Ω_λ were introduced before (see eqs 11 and 18).

Once $\mathbf{a}^J$ is calculated, eq 3 is used to calculate the required $S(\nu\leftarrow\lambda)$ element. For this sake we substitute eqs 15, 23, and 32, integrate over R_ν, r_1, and r_2, and sum over all the randomly related sets of three Jacobi angles (γ_1, γ_2, δ). The relevant state-to-state cross sections are calculated from the expression

$$\sigma(v\bar{j}v'\leftarrow n_1j_1n_2j_2) = [\pi/k^2(n_1j_1n_2j_2)]\sum_J (2J+1)|S_J(v\bar{j}v'\leftarrow n_1j_1n_2j_2)|^2 \quad (38)$$

where

$$k(n_1j_1n_2j_2) = [(2\mu_\nu/\hbar^2)(E - \epsilon_{n_1j_1} - \epsilon_{n_2j_2})]^{1/2} \quad (39)$$

Here $\epsilon_{n_ij_i}$ ($i = 1, 2$) are (initial) eigenvalues of the two asymptotic diatoms.

III. Numerical Details

As specified, the numerical treatment was performed for the exchange process

$$H_2(v_H) \rightarrow OX(v_0) \rightarrow HOX(v\bar{j}v') + H \quad (X = H, D)$$

We report on state-to-state cross sections for three different initial states, namely, (0,0), (0,1) and (1,0) and for ~20 final states where the range of $v(v')$ is (0, ..., 3) and the range of $\bar{j}$ is (0, ..., 6). To carry out the calculations, the translational coordinate R_ν was divided by 30–35 equidistant division points. To each point was attached one exponential as a translational basis function and a set of vibrational adiabatic basis functions. The number of these functions varied from one division point to the other and was determined by a given energy value (see discussion in ref 6e). The range of R_ν was divided into two regions: the one along

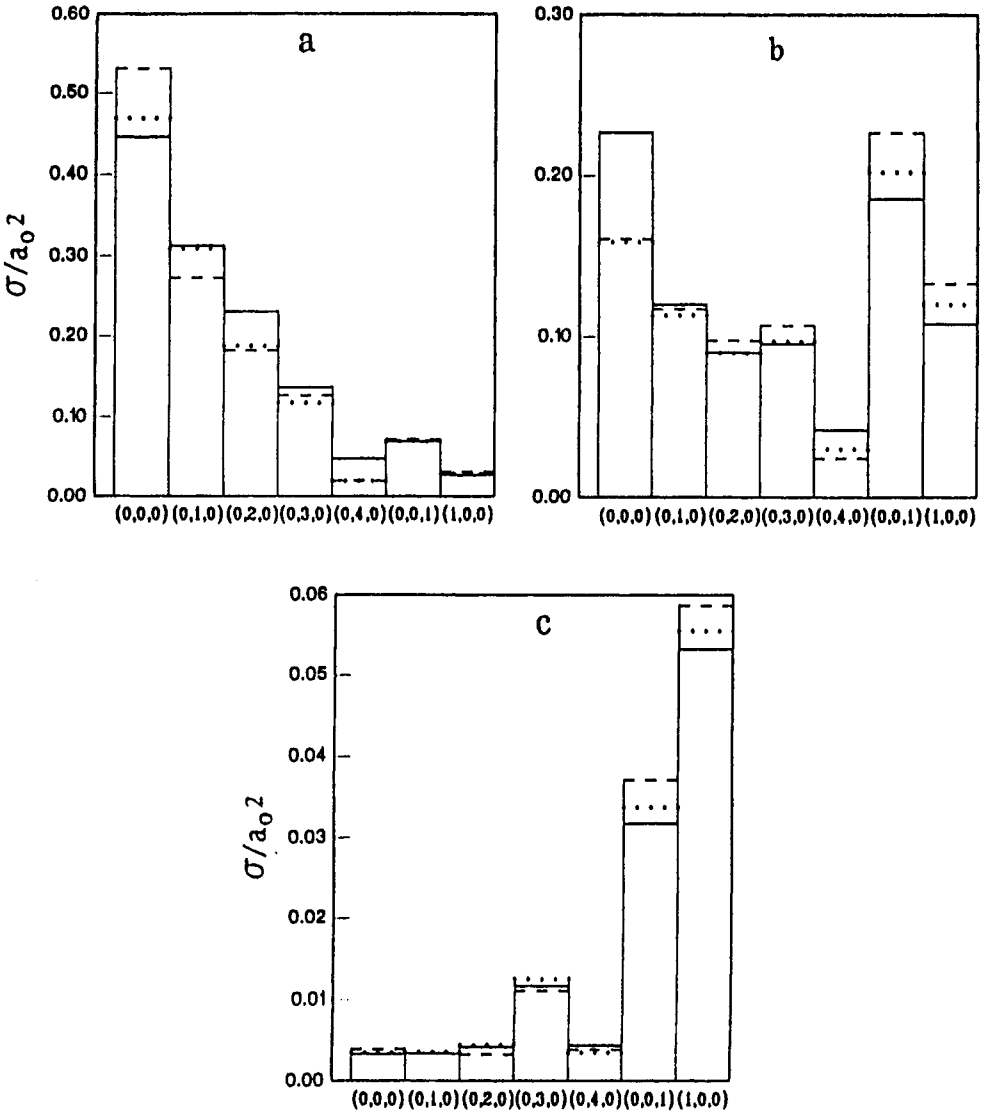

Figure 3. Convergence study with respect to the number of sets of Jacobi's γ_1, γ_2, and δ angles. State-to-state cross sections for the processes (a) $H_2(0) + OH(0) \rightarrow HOH(v\bar{j}v'|K=0) + H$ (E_{tr} = 0.700 eV), (b) $H_2(1) + OH(0) \rightarrow HOH(v\bar{j}v'|K=0) + H$ (E_{tr} = 0.203 eV), and (c) $H_2(0) \rightarrow OH(1) \rightarrow HOH(v\bar{j}v'|K=0) + H$ (E_{tr} = 0.275 eV). (- - -) Calculations based on 28 Monte-Carlo randomly selected sets of γ_1, γ_2, and δ. (···) As for (- - -) but with 33 sets. (—) As for (- - -) but with 38 sets.

which the NIP was defined (this region is located in the asymptotic part of R_ν) and the other where the NIP was identically zero. In the present treatment, the whole range of R_ν was 1.0–4.5 Å, and the one along which the NIP is different from zero was $[R_I, R_I + \Delta R_I] \equiv$ [3.8–4.5 Å]. The height of the NIP, namely, V_{10R}, was 0.6 eV.

The following distinction was made for the two vibrational coordinates r_1 and r_2. The range for the reactive bond was assumed to be 0.4–3.2 Å whereas the range for r_2—the nonreactive bond—was taken as 0.5–1.8 Å.

The size of the matrix to be calculated and inverted in each case depended on the total energy and on the mass of the X atom (whether H or D). Usually these sizes were in the range of 300–600.

These inversions had to be done for each value of J and each set of three angles (γ_1, γ_2, δ). The range from J_{max} was 30–45, again depending on the energy and the X mass. As for the Monte-Carlo selected angles, the calculations were based on ~40 sets which were distributed among three groups to enhance convergence. Each group was attached to a geometrical region in configuration space. The size of these regions was determined according to their relative contributions to the cross sections (a fourth region, the largest by far, was excluded altogether, as it was found, after a careful study, that no reactions originated from there). For instance, it was realized that in the low-energy region most of the reactive interactions were from quasi-collinear configurations. Contributions from other configurations became more frequent as the energy increased.

A large number of computer runs were performed in order to determine the optimal set of parameters to carry out the calculations (a similar study is described in ref 6e for the triatom system). In the present paper we will refer only to the rate of convergence of the state-to-state cross sections with regard to the number of sets of Jacobi angles (γ_1, γ_2, δ). This study is presented in Figure 3 and Table 1. In general 40 sets of these angles were required to achieve convergence within 10%.

Before showing and discussing the results, we present in Figure 2 a diagram of the initial and final states for the HHOH and HHOD systems. Its main features are the exothermicities which are ~0.5 eV for the (0,0) initial state and ~1.0 eV for the (1,0) and (0,1) states.

IV. Results and Discussion

Integral cross sections for the two processes

$$XO(0) + H_2(0) \rightarrow XOH(K=0) + X \quad (X = H, D) \qquad (Ia)$$

as a function of translational energy are shown in Figure 4.

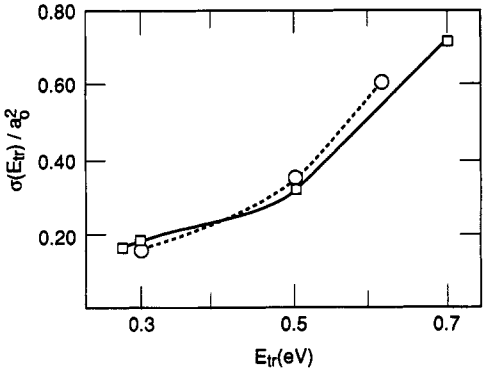

Figure 4. Total reactive cross sections as a function of translational energy for the systems $H_2(0) + OH(1) \rightarrow H_2O(K=0) + H$ and $H_2(0) + OD(0) \rightarrow HDO(K=0) + H$.

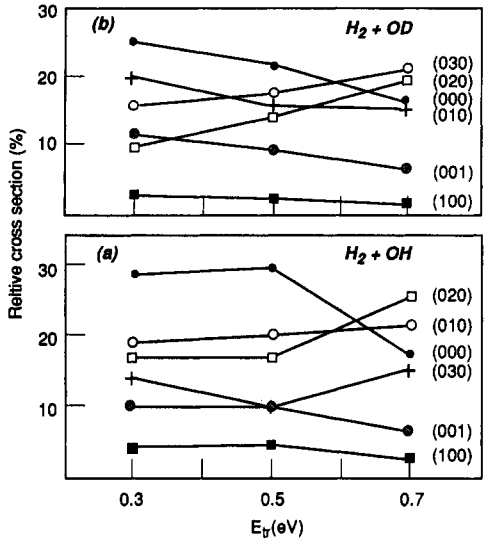

Figure 5. Relative state-to-state cross sections (%) as a function of translational energy: (a) $H_2(0) + OH(0) \rightarrow H_2O(v\bar{j}v'|K=0) + H$, (b) $H_2(0) + OD(0) \rightarrow HDO(v\bar{j}v'|K=0) + H$.

TABLE 1: Convergence Study with Respect to the Number of Sets of the Three Jacobi Angles γ_1, γ_2, and δ: State-Selected Integral Cross Sections (a_0^2) for the Reactions $H_2(v) + OH(v') \rightarrow H_2O(K=0) + H$

initial state		translational			
v	v'	energy (eV)	28 sets	33 sets	38 sets
0	0	0.700	0.64	0.64	0.70
1	0	0.203	0.50	0.52	0.58
0	1	0.275	0.18	0.18	0.22

Interestingly, no isotopic effect is detected; the cross sections for the two processes are indentical within the accuracy of the calculation. Product distributions for the two systems are shown in Figure 5, as a function of translational energy. As for the HHOH system, with only a few exceptions, no inversion processes are observed; namely, the lower the respective eigenstate, the higher its population. Moreover, hardly any selectivity is seen with respect to the two internal vibrational motions. A somewhat different situation is encountered for the HHOD system. Here the nice order concerning the relative populations of the various states obtained for the HHOH system is not preserved anymore. This is true not only for the highest energy but even for the lower energies. The most prominent case is the (100) state which along the whole studied energy range is much less populated than the (001) and (030) states, although both these states are energetically higher (it is important to emphasize that in the notation (vxv') for the DOH molecule, v stands for the OD local mode and v' for the OH local mode, whereas for the HOH molecule, v stands for the asymmetric mode and v' for the symmetr ic mode). This

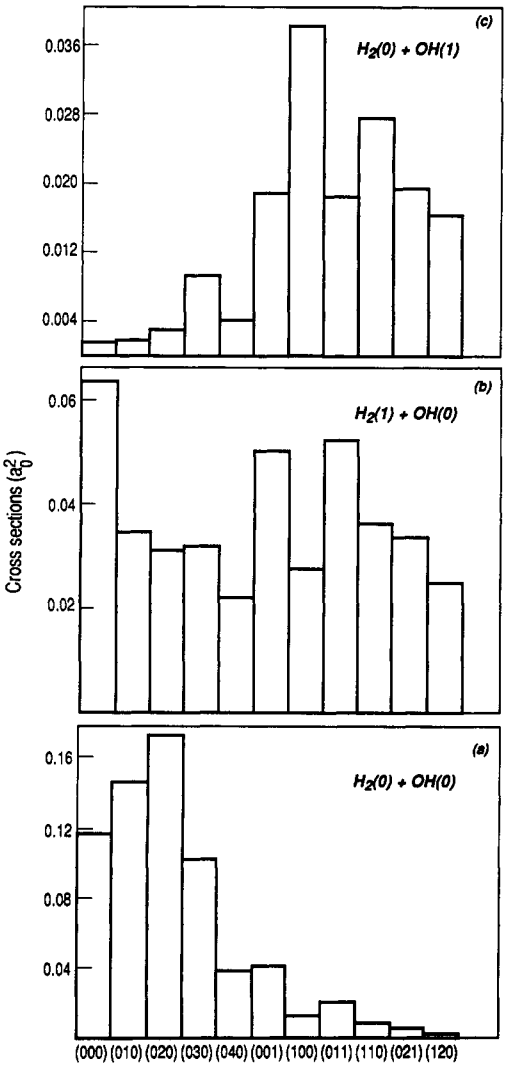

Figure 6. State-to-state cross sections as calculated for $E_{tot} = 1.181$ eV: (a) $H_2(0) + OH(0) \rightarrow H_2O(v\bar{j}v'|K=0) + H$ ($E_{tr} = 0.700$ eV), (b) $H_2(1) + OH(0) \rightarrow H_2O(v\bar{j}v'|K=0) + H$ ($E_{tr} = 0.203$ eV), (c) $H_2(0) + OH(1) \rightarrow HOH(v\bar{j}v'|K=0) + H$ ($E_{tr} = 0.275$ eV).

fact has to do with adiabaticity of the nonreactive (OD) bond in this system as was discussed previously[1e-h,2] (we shall return to this subject later).

Another feature to emerge from the calculations is the fact that the relative populations of the (000) state in both systems decrease as a function of energy at the expense of the population of the higher bend states (the relative populations of the two vibrational modes are only slightly affected by the energy increase).

In Figures 6 and 7 are shown the final product state distributions for a fixed *total* energy (but for different translational (or internal) energies of the reactants). The results for the HHOH system are presented in Figure 6 for $E_{tot} = 1.181$ eV and those for the HHOD system in Figure 7 for $E_{tot} = 1.026$ eV (the translational energies for the various initial states are given in Table 2). It can be seen that the initial states of the reagents have a strong effect on the product distributions. Whereas when the reagents are in their ground states most of the product molecules are formed in the low bend states (see Figures 6a and 7a), exciting the vibrational states of one of the interacting molecules yields a high percentage of the products in vibrationally excited modes (see Figures 6b,c and 7b,c). These facts are well known for the reagent excited OD molecule and the product DOH molecule. The explanation is based on two features: (a) the OD bond is preserved during the reaction process and (b) the vibrational modes of the DOH molecule are local modes. Consequently the energy, originally

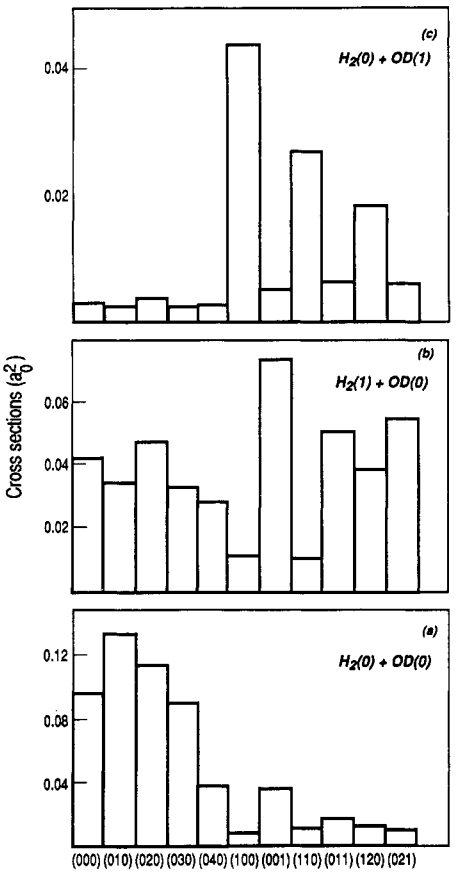

Figure 7. Same as Figure 6 but for E_{tot} = 1.026 eV and the following reactions: (a) $H_2(0) + OD(0) \rightarrow DOH(v\bar{j}v'|K=0) + H$ (E_{tr} = 0.613 eV), (b) $H_2(1) + OD(0) \rightarrow DOH(v\bar{j}v'|K=0) + H$ (E_{tr} = 0.116 eV), (c) $H_2(0) + OD(1) \rightarrow DOH(v\bar{j}v'|K=0) + H$ (E_{tr} = 0.300 eV).

TABLE 2: Eigenvalues (eV) and Translational and Total Energies (eV) for the H_2 + OX (X = H, D) Systems (Numbers Relevant to Figures 6 and 7)

		H_2 + OH			H_2 + OD		
v	v'	eigenvalue	translational energy	total energy	eigenvalue	translational energy	total energy
0	0	0.481	0.700	1.181	0.413	0.613	1.026
0	1	0.906	0.275	1.181	0.726	0.300	1.026
1	0	0.978	0.203	1.181	0.910	0.116	1.026

stored in the OD bond, moves smoothly into the OD local mode of the DOH molecule. (Such selectivities were observed also in other kinds of studies[15].) The situation changes (but only slightly) when it comes to the vibrationally excited OH molecule. Here, like before, the OH bond is preserved during the reaction process, but although the (low) vibrational modes of the HOH molecule are not local (as was explicitly shown in our previous study[2j] and also in ref 14), the energy still remains in the vibrational modes, although this time it is distributed between the symmetric and the asymmetric modes of the HOH product molecule. Thus, like in the DOH case, most of the products are formed in vibrationally excited HOH states, but the final distribution between the two modes is determined by statical considerations that follow from Franck–Condon-type models.[16]

It is now well accepted that exciting the OD bond will have only a minor effect on the reaction process[1e-h,2] and that consequently the distribution of the final bend modes will, at most, be only slightly affected. This is illustrated in Figure 8a, where the relative bend distributions $P(0,j,0)$ that follow from the reaction $H_2(0) + OD(0) \rightarrow DOH + H$ are compared with the sum of the two (relative) distributions $P(0,j,1) + P(1,j,0)$ that follow from the reaction $H_2(0) + OD(1) \rightarrow DOH + H$. The two calculations were carried out for the same translational energy,

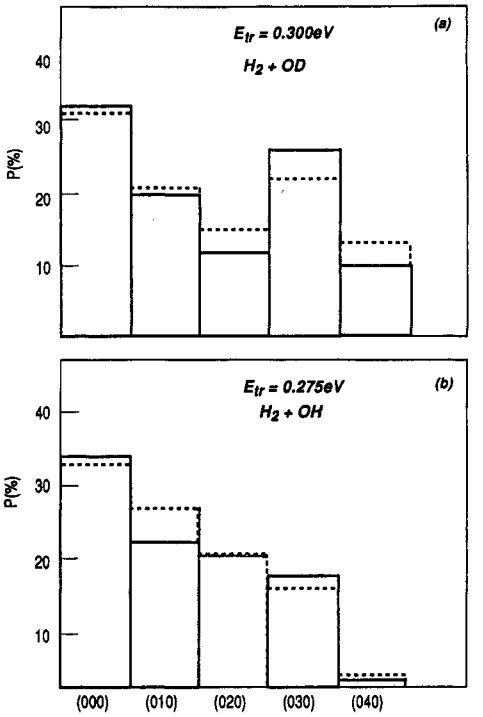

Figure 8. Relative cross sections as a function of the bend quantum number $\bar{j}$: (a) (—) cross sections for $H_2(0) + OD(0) \rightarrow DOH(0\bar{j}0|K=0) + H$, (- - -) sum of the cross sections for the two processes

$$H_2(0) + OD(1) \rightarrow \begin{cases} HOD(0\bar{j}1|K=0) \\ HOD(1\bar{j}0|K=0) \end{cases} + H$$

calculations were done for E_{tr} = 0.300 eV; (b) like (a) but for the H_2 + OH system r, calculations were done for E_{tr} = 0.275 eV.

TABLE 3: Comparison between Cross Sections (a_0^2) Calculated for the Reactions $H_2(0) + OX(v_0) \rightarrow XOH(K=0) + H$ (X = H, D) at Fixed Translational Energies[a]

v_0	HOHH	HHOD
0	0.178	0.188
1	0.22	0.22

[a] The calculations for the HHOH system were done at E_{tr} = 0.275 eV and those for HHOD at E_{tr} = 0.3 eV.

i.e., E_{tr} = 0.3 eV. It is seen that the two distributions are almost identical (note the nice fit for j = 3 in particular). The question is whether this similarity is because the DOH molecule has local modes or whether this is a general feature which results from the adiabaticity of the nonreactive bond. In Figure 8b we show the relevant bend distributions for the $H_2(0) + OH(v_0) \rightarrow HOH + H$ (v_0 = 0, 1) processes (this time the two calculations were done for E_{tr} = 0.275 eV), and again, as before, the two distributions are similar. This shows that the similarity in the bend distributions results from the adiabaticity of the nonreactive bond.

More about the similarity between the two isotopic reactions is presented in Table 3 where the total cross sections for two different initial vibrational states of the OX (X = H, D) molecules, calculated at the same translational energies (the calculations for the HHOH system were carried out at E_{tr} = 0.275 eV and those for the HHOD system at E_{tr} = 0.3 eV), are compared. In general the four cross sections are similar to each other (the lower cross sections for the HHOH system are due to the lower translational energy and consequently are more markedly affected by the potential barrier).

Part of our study was also devoted to the influence of a vibrationally excited H_2 molecule on the reaction process. In Table 4 are given the total cross sections for the processes $H_2(v_H) + OX(0) \rightarrow XOH + H$ (X = H, D; v_H = 0, 1) (the calculations for the HHOH system were done at E_{tot} = 1.181 eV and those

TABLE 4: Comparison between Cross Sections (a_0^2) Calculated for the Reactions $H_2(v_H)$ + OX(0) → XOH(K=0) + H (X = H, D) at Fixed Total Energies[a]

v_H	HOHH	HHOD
0	0.70	0.60
1	0.58	0.66

[a] The calculations for the HHOH system were carried out at E_{tot} = 1.181 eV and those for the HHOD system at E_{tot} = 1.026 eV.

for the HHOD system at E_{tot} = 1.026 eV). In general the four cross sections are similar to each other.

These two modes affect the final state distribution of the products much more markedly. Whereas in the case of the H_2 ground state most of the products are formed in the low bend modes (see Figures 6a and 7a), large fractions of vibrationally excited XOH molecules are obtained in the case of the excited H_2. Here we encounter what is known as the $v \rightarrow v'$ transition law, mentioned frequently for atom–diatom systems.[16] In other words although the H_2 bond is the reactive bond, most of the energy stored in this bond moves into the vibrational modes of the product XOH molecule. In the case of the HHOD system this energy is stored solely in the newly formed HO bond (this again is due to the adiabaticity of the OD bond), and in the case of the HHOH this energy is mainly stored in the symmetric mode; however, a large fraction of it is also found in the asymmetric mode.

As was mentioned several times throughout this paper, similar studies were performed by other groups. We are not in a stage of conducting systematic comparisons with results obtained from other approaches because, so far, we considered state-to-state cross sections for one final (total) rotational state, K, i.e., K = 0. Nevertheless, a few remarks can be made.

(*a*) *Integral Cross Sections.* We didn't find any isotopic effect by replacing an H atom in the OH molecule by a D atom. This is very similar to what was found by Clary in his QM study.[2h] We have a preliminary result for total cross section at E = 0.3 eV, and we found it to be somewhat smaller than the QCT result of Schatz and Elgersma[2a] (SE) and the semiclassical result of Billing but much smaller than Clary's QM result.[2d]

(*b*) *Internal State Distributions.* We found the product molecules (H_2O or DOH) to be primarily rotationally (namely, bend states) excited, and only *a small* fraction of them were excited vibrationally. This is in accordance with the semiclassical results of Billing,[2d] in partial contradiction to the QCT results of SE[2a] and in contradiction to the QM results of Clary.[2h] Again judging from our preliminary full treatment, the strong preference of exciting bend states is encountered in all other K states as well.

V. Conclusions

In this work we calculated reactive cross sections for the two processes given in reaction I. We limited ourselves to the lowest (products) rotational state (K = 0) of the triatom product molecule mainly for the purpose of gaining physical insight into the general diatom–diatom reactive process (the $K \neq 0$ cross sections and the total cross sections will be published elsewhere).

In what follows we summarize the numerical procedure, emphasizing the approximations that were done. Within the numerical treatment we distinguish between three different calculations: (1) The calculation of ψ_{0v} which is the unperturbed (asymptotic) wave function of the reagents—the two diatomics. The function ψ_{0v} describes an elastic scattering process. (2) The calculation of $\psi_{0\lambda}$ which is the unperturbed (asymptotic) wave function of the products—the atom and the triatom. Like ψ_{0v}, the function $\psi_{0\lambda}$ describes an elastic scattering process. (3) The calculation of χ_λ which is the perturbed part of the total wave function calculated in the enlarged reagent (or product) AC.

The two functions $\psi_{0\lambda}$ and ψ_{0v} are treated in their full dimensionality (which also means keeping all relevant quantum numbers); namely, the functions are described employing all six internal coordinates. However, to reduce the computational efforts, we did not use the Arthurs–Dalgarno representation[17] but the one within the j_z approximation. The χ_λ function is also expressed in terms of all six coordinates but is treated within the breathing-sphere approximation. Here the three angles γ_1, γ_2, and δ are considered as parameters of the potential rather than variables, and consequently for each separate calculation the potential becomes isotropic. S matrix elements were obtained for 45 different randomly selected sets of such angles. The final cross sections are calculated, averaging over these angles. Although it was a relatively heavy calculation, we significantly reduced the amount of programming and computer time by applying NIPs to decouple reactive ACs.

The two isotopic reactions which were considered differ in that the two product–triatom molecules have different vibrational modes: the HOH molecule is characterized by normal modes,[2j,14] whereas the DOH molecule is characterized by local modes.[2j] Although their internal structure was different, we could observe no significant isotopic effects on the reaction process. The magnitude of the total cross sections (for K = 0) as a function of translational energy were similar, and the overall internal distributions were almost the same. It is true that, in the OD(1) case, the (1,0,0) state was by far the most populated one (hardly any products were detected in the (0,0,1) state), whereas in the case of OH(1) the two vibrational states (1,0,0) and (0,0,1) were almost equally populated. Still, the sum of the transition probabilities of the two vibrationally excited states was equal to those of the DOH molecule. We also studied the effect of a vibrationally excited H_2 molecule on the reaction process and were able to establish the (proper) $v \rightarrow v'$ transition law for the tetraatom system in question.[18]

Acknowledgment. This work was supported by the US-Israel Binational Science Foundation and the Israel Academy of Sciences and Humanities.

References and Notes

(1) (a) Light, G. C.; Matsumoto, J. H. *Chem. Phys. Lett.* **1978**, *58*, 578. (b) Zellner, R.; Steinert, W. *Chem. Phys. Lett.* **1981**, *81*, 568. (c) Glass, G. P.; Chaturvedi, B. K. *J. Chem. Phys.* **1988**, *75*, 2749. (d) Kleinermanns, K.; Wolfrum, J. *Appl. Phys. B* **1984**, *34*, 5. (e) Sinha, A.; Hsiao, M. C.; Crim, F. F. *J. Chem. Phys.* **1990**, *92*, 6333. (f) *Ibid.* **1991**, *94*, 4928. (g) Sinha, A. *J. Phys. Chem.* **1990**, *94*, 4391. (h) Bronikowski, M. J.; Simpson, W. R.; Girard, B.; Zare, R. N. *J. Chem. Phys.* **1991**, *95*, 8647. (i) Alagia, M.; Bolucani, N.; Casaveccia, P.; Stranges, D.; Volpi, G. G. *J. Chem. Phys.* **1993**, *98*, 2459.

(2) (a) Schatz, G. C.; Elgersma, H. *Chem. Phys. Lett.* **1980**, *73*, 21. (b) Schatz, G. C.; Colton, M. C.; Grant, J. L. *J. Phys. Chem.* **1988**, *88*, 2971. (c) Truhlar, D. G.; Isaacson, A. D. *J. Chem. Phys.* **1982**, *77*, 3516; **1982**, *76*, 1380. (d) Billing, G. D. *Chem. Phys.* **1990**, *146*, 63. (e) Rashed, O.; Brown, N. J. *J. Chem. Phys.* **1985**, *82*, 5506. (f) Harrison, J. A.; Mayne, H. R. *J. Chem. Phys.* **1988**, *88*, 7424. (g) Clary, D. C. *J. Chem. Phys.* **1991**, *95*, 7298. (h) Clary, D. C. *Chem. Phys. Lett.* **1992**, *192*, 34. (i) Kudla, K.; Schatz, G. C. *Chem. Phys. Lett.* **1992**, *193*, 507. (j) Szichman, H.; Last, I.; Baram, A.; Baer, M. *J. Phys. Chem.* **1993**, *97*, 6436.

(3) (a) Walch, S. P.; Dunning, T. H. *J. Chem. Phys.* **1980**, *72*, 1303. (b) Schatz, G. C.; Walch, S. P. *Ibid.* **1980**, *72*, 776. (c) Schatz, G. C. Private communications.

(4) (a) Baer, M.; Ng, C. Y. *J. Chem. Phys.* **1990**, *93*, 7789. (b) Johnson, B. R. *J. Chem. Phys.* **1986**, *84*, 176.

(5) Neuhauser, D.; Baer, M. *J. Chem. Phys.* **1989**, *90*, 4351; **1989**, *91*, 4651; **1990**, *92*, 3419.

(6) (a) Baer, M.; Neuhauser, D.; Oreg, Y. *J. Chem. Soc. Faraday Trans* **1990**, *86*, 1721. (b) Baer, M.; Nakamura, H. *J. Chem. Phys.* **1992**, *96*, 6565. (c) Last, I.; Baer, M. *Chem. Phys. Lett.* **1992**, *189*, 84. (d) Last, I.; Baram, A.; Baer, M. *Chem. Phys. Lett.* **1992**, *169*, 534. (e) Last, I.; Baram, A.; Szichman, H.; Baer, M. *J. Phys. Chem.* **1993**, *97*, 7040.

(7) Wu, T. Y.; Ohmura, T. *Quantum Theory of Scattering*; Prentice-Hall: Englewood Cliffs, NJ, 1962.

(8) (a) McGuire, P.; Kouri, D. J. *J. Chem. Phys.* **1974**, *60*, 2488. (b) Pack, R. T. *J. Chem. Phys.* **1974**, *60*, 633. (c) Tamir, M.; Shapiro, M. *Chem. Phys. Lett.* **1975**, *31*, 166. (d) Heil, T. G.; Green, S.; Kouri, D. J. *J. Chem. Phys.* **1978**, *68*, 2562.

(9) Shima, Y.; Baer, M. *J. Phys. B* **1983**, *16*, 2169.

(10) Tennyson, J.; Sutcliffe, B. T. *J. Chem. Phys.* **1982**, *77*, 4061.

(11) (a) Heller, E. J.; Yamani, H. A. *Phys. Rev. A* **1974**, *9*, 1201, 1209. (b) Rescigno, T. N.; Reinhardt, W. P. *Phys. Rev. A* **1973**, *8*, 2828. (c) Miller,

W. H.; Jensen-Op-der Haar, B. M. D. D. *J. Chem. Phys.* **1986**, *86*, 6213. (d) Zhang, J. Z. H.; Chu, S. I.; Miller, W. H. *J. Chem. Phys.* **1988**, *88*, 6233.

(12) (a) Bacic, Z.; Light, J. C. *J. Chem. Phys.* **1986**, *85*, 4595; **1987**, *86*, 3065. (b) Zhang, J. Z. H.; Miller, W. H. *J. Phys. Chem.* **1990**, *94*, 7785. (c) Zhang, J. Z. H. *Chem. Phys. Lett.* **1991**, *181*, 63.

(13) Rose, M. E. *Elementary Theory of Angular Momentum*; John Wiley and Sons: New York, 1957; Chapter IV.

(14) Lawton, R. T.; Child, M. S. *Mol. Phys.* **1980**, *40*, 773.

(15) Hartke, B.; Manz, J.; Mathis, J. *Chem. Phys.* **1989**, *139*, 123. Hartke, B.; Manz, J. *J. Chem. Phys.* **1989**, *92*, 220.

(16) Baer, M. *J. Chem. Phys.* **1974**, *60*, 1057; *J. Phys. Chem.* **1981**, *85*, 3974. Halavee, U.; Shapiro, M. *J. Chem. Phys.* **1976**, *64*, 2826. Schatz, G. C.; Ross, J. *J. Chem. Phys.* **1977**, *66*, 1021, 1037.

(17) Arthurs, A. M.; Dalgarno, A. *Proc. R. Soc. London* **1960**, *A256*, 540.

(18) See for instance: Abu Salbi, N.; Kouri, D. J.; Shima, Y.; Baer, M. *J. Chem. Phys.* **1985**, *82*, 2650.